A Statistics-Based Material Property Analysis to Support TPS Characterization

Sean R. Copeland*
Stanford University, Stanford, CA 94305, U.S.A.

Ioana Cozmuta†
ERC Inc., NASA Ames Research Center, Moffett Field, CA 94035, U.S.A.

Juan J. Alonso‡
Stanford University, Stanford, CA 94305, U.S.A.

Accurate characterization of entry capsule heat shield material properties is a critical component in modeling and simulating Thermal Protection System (TPS) response in a prescribed aerothermal environment. The thermal decomposition of the TPS material during the pyrolysis and charring processes is poorly characterized and typically results in large uncertainties in material properties as inputs for ablation models. These material property uncertainties contribute to large design margins on flight systems and cloud reconstruction efforts for data collected during flight and ground testing, making revision to existing models for entry systems more challenging. The analysis presented in this work quantifies how material property uncertainties propagate through an ablation model and guides an experimental test regimen aimed at reducing these uncertainties and characterizing the dependencies between properties in the virgin and charred states for a Phenolic Impregnated Carbon Ablator (PICA) based TPS. A sensitivity analysis identifies how the high-fidelity model behaves in the expected flight environment, while a Monte Carlo based uncertainty propagation strategy is used to quantify the expected spread in the in-depth temperature response of the TPS. An examination of how perturbations to the input probability density functions affect output temperature statistics is accomplished using a Kriging response surface of the high-fidelity model. Simulations are based on capsule configuration and aerothermal environments expected during the Mars Science Laboratory (MSL) entry sequence. We identify and rank primary sources of uncertainty from material properties in a flight-relevant environment, show the dependence on spatial orientation and in-depth location on those uncertainty contributors, and quantify how sensitive the expected results are.

Nomenclature

c_p	Specific Heat
C_H	Convective Heat Transfer Coefficient
EDL	Entry, Descent and Landing
$\dot{m}$	Mass Flow Rate
$HEAT$	Hollow aErothermal Ablation Temperature Sensor
$MEADS$	Mars Entry Atmospheric Data System
$MEDLI$	Mars Entry Descent and Landing Instrumentation
$MISP$	MEDLI Integrated Sensor Plug
MSL	Mars Science Laboratory

*Ph.D. Candidate, Department of Aeronautics & Astronautics, AIAA Student Member.
†Senior Research Scientist, Aerothermodynamics Branch, Member AIAA.
‡Associate Professor, Department of Aeronautics & Astronautics, AIAA Senior Member.

$PICA$	Phenolic Impregnated Carbon Ablator
q	Heat Rate
$\dot{s}$	Surface Recession Rate
T	Temperature
TC	Thermocouple
TPS	Thermal Protection System
u_e	Boundary Layer Edge Velocity
x	Coordinate System Moving with Recessing Surface
y	Fixed Coordinate System
α	Absorptivity
ϵ	Emissivity
Γ	Resin Volume Fraction
κ	Thermal Conductivity
μ	Population mean
σ	Population standard deviation
ρ	Density
θ	Time

Subscript

A	Resin constituent A
B	Resin constituent B
C	Ablator Reinforcing Material C
c	Char
g	Pyrolysis Gas
R	Radiation
v	Virgin
w	Wall or Surface

I. Introduction

A. Background

Vehicles traveling at hypersonic speeds through planetary atmospheres generate flowfields characterized by strong shocks generating very high temperatures that can lead to chemical and thermodynamic non-equilibrium.[1] Significant amounts of heat are transferred from the surrounding flow to the vehicle through one, or a combination of many, of the following modes: convection, chemical recombination, and radiation. The contributions to surface heating from each of these modes are dominated by the details of the specific problem in question and are consequences of the vehicle configuration and mission profile. To survive the harsh environmental conditions, hypersonic vehicles require the use of Thermal Protection Systems (TPS). The materials used in these systems manage the heat transfer to the vehicle substructure by withstanding very high surface temperatures, re-radiating energy back to the surrounding atmosphere and, in some cases, rejecting energy through ablation.

Design and analysis of entry vehicle TPS utilizes a combination of ground-based experimental testing in conjunction with high-fidelity modeling and simulation, though both of these approaches have limitations. Ground-based testing is unable to replicate all aspects of the flight environment, creating challenges in extrapolating these experiments to flight conditions, while simulation requires modeling of many complex physical phenomena (including surface chemical catalysis, shock-layer radiation, roughness-induced turbulent transition, pyrolysis gas blowing in the boundary layer, thermal decomposition of the TPS material, and many more). Two primary sources of uncertainty exist: uncertainty in model parameters due to natural (aleatory) variation in the system, and errors from poor capturing of the physical phenomena by the form of the governing equations (epistemic). Aleatory uncertainties in heat shield performance metrics can arise from many sources, including system operating conditions, entry trajectory dispersion, aerothermal environments, and TPS material properties.[9] Model form uncertainties have been difficult to identify and correct, due in large part to a general sparsity of flight test data available for verification and validation efforts. These large uncertainties contribute to a lack of confidence in the results of high-fidelity, coupled entry simulations,

resulting in the application of large *ad hoc* margins based on expert opinion that are aligned with the level of acceptable risk of the program. The large margins, and poor understanding of the aerothermal environment have implications on crew safety, mission success, and scientific return from planetary entry systems. To address this issue, NASA has included a suite of instruments embedded in the Mars Science Laboratory heat shield that will collect data during the entry phase of its mission, returning it to scientists and engineers on Earth upon its landing on the Martian surface.

B. Mars Science Laboratory - MEDLI

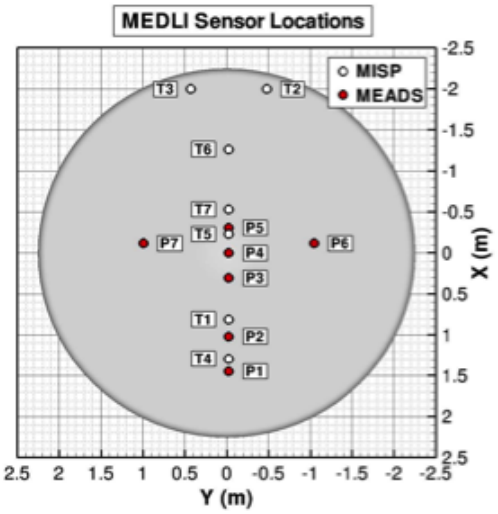

Figure 1. Locations of the MEADS and MISP System. From Ref. ([10]).

The Mars Science Laboratory Entry, Descent, and Landing Instrumentation (MEDLI) program[3] consists of a network of seven Mars Entry Atmospheric Data System (MEADS) pressure sensors and seven MEDLI Integrated Sensor Plugs (MISPs) distributed strategically on the surface of the MSL heat shield. The program, if successful, will return the largest flight-relevant dataset from the Martian atmosphere in history, and will provide insight to the aerothermal environment, the Martian atmosphere and in-depth performance of the MSL heat shield. The data returned from the program will be crucial to the design of future planetary missions and to the validation of thermo-physical models.

The embedded MISPs consist of four Type-K thermocouples at various depths in the plug (nominally 0.1", 0.2", 0.45", and 0.7" below the surface) and a Hollow aErothermal Ablation and Temperature (HEAT) sensor. The four thermocouples return temperature data in time at the four specified depths for each of the 7 MISP locations while the HEAT sensor tracks the progression of an isotherm through the TPS material. A comparison of the data with the predictions from the ablation model will determine if the model in place appropriately captures the thermal decomposition and ablation process. Once validated, a calibration of the model to match the experimental results will yield a reconstruction of the imposed heating at the MISP locations and support other MEDLI Science Requirements.

It is critical to characterize the material properties of the sensor plug as closely as possible. Uncertainties in these properties will cloud the reconstruction and model validation effort, and could lead to erroneous conclusions when leveraging analysis tools to draw inferences necessary to to support the program objectives. A dedicated test effort is being planned to address this issue in detail, identifying and quantifying material property uncertainties as best as possible, with the goal of constructing a refined PICA material model for use in the predictive simulations.

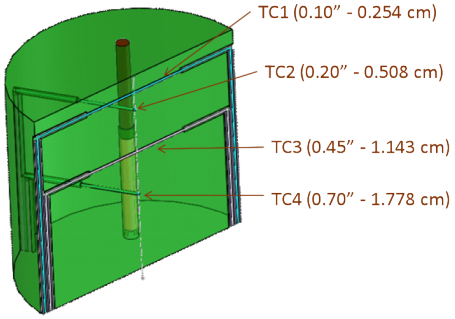

Figure 2. MISP cutaway showing in-depth sensor placement.

II. Model

The analysis presented in this paper is the processed output of a software package developed at the NASA Ames Research Center called the Fully Implicit Ablation and Thermal Analysis Program (FIAT).[5] FIAT is based on a software package called CMA, developed in the 1960s by the Aerotherm Corporation.[7] CMA has been widely used in the aerospace community for the analysis of ablating heatshields during atmospheric entry for many decades, but suffered from convergence issues tied to grid spacing and time-stepping due to the explicit coupling of its governing equations. FIAT solves these governing equations with a fully implicit approach, greatly improving the convergence properties of the simulations. Combined with the recent work to improve the material models, FIAT represents the state-of-the-art in ablation modeling

and has been used in the analysis and design processes for many NASA missions.

FIAT solves a system of four coupled partial differential equations. These equations are outlined below to give the reader a perspective of the physical equations used to model the ablation process, but are augmented with numerous supporting equations to model specific terms in these governing equations. These supporting equations and models are omitted for brevity, but can be found in the original source material for FIAT.[6]

A. Internal Energy Balance Equation

The internal energy balance equation is a transient thermal conduction problem with radiation and pyrolysis contributions:

$$\rho c_p \left.\frac{\partial T}{\partial \theta}\right|_x = \frac{\partial}{\partial x}\left(\kappa \frac{\partial T}{\partial x} - q_R\right)_\theta + \left(h_g - \bar{h}\right)\left.\frac{\partial \rho}{\partial \theta}\right|_y + \dot{s}\rho c_p \left.\frac{\partial T}{\partial x}\right|_\theta + \dot{m}_g \left.\frac{\partial h_g}{\partial x}\right|_\theta. \tag{1}$$

As the ablator material pyrolyzes, chars, and subsequently ablates, the surface of the material recedes. The x coordinate moves with this ablation front, while the y axis remains fixed. The terms in Eq. (1) can be interpreted as: the accumulation of sensible energy, net rate of conduction and radiative heat fluxes, rate of energy consumed during the pyrolysis process, convection rate of sensible energy due to a moving coordinate system, and the rate of energy convection from pyrolysis gas.

B. Internal Decomposition Equation

The ablator material is modeled as a three component composite material, where two materials A and B for the resin filler are mixed with a reinforcing material C in a volume fraction dictated by the input parameter Γ:

$$\rho = \Gamma\left(\rho_A + \rho_B\right) + \left(1 - \Gamma\right)\rho_C. \tag{2}$$

Each component decomposes independently according to a model based on an activation temperature for each constituent.

C. Internal Mass Balance Equation

As ablator material thermally decomposes, its density changes from that of the virgin material to a less-dense charred state, producing pyrolysis gasses that are ejected from the material into the surrounding flowfield. The continuity equation captures this mass transfer by assuming quasi-1D flow and an impermeable substructure:

$$\frac{\partial \dot{m}_g}{\partial y} = \frac{\partial \rho}{\partial \theta}. \tag{3}$$

D. Surface Energy Balance Equation

The surface energy balance dictates the heating to the TPS material due to the imposed aerothermal environment, capturing convective, radiative, and surface thermochemical effects between the ablator and the surrounding flowfield:

$$\rho_e u_e C_H\left(H_r - h_w\right) + \dot{m}_c h_c + \dot{m}_g h_g + \alpha q_{rad} = \left(\dot{m}_c + \dot{m}_g\right) h_w + \sigma \epsilon_w T_w^4 + q_{cond}. \tag{4}$$

Left hand side terms represent the contributions to the surface energy rate while the right hand side terms reject heat from the surface. Contributors the the surface energy include the sensible convective heat flux, the contribution to surface heat flux due to the moving coordinate system, the energy from the escaping pyrolysis gas, and the incoming radiative heat flux. Rejection of energy from the surface is due to energy released from the ablation process, energy re-radiated to the surrounding flowfield, and conduction into the the heatshield material. The convective heat transfer coefficient C_H employs a correction to account for the blowing of pyrolysis gasses at the surface.

E. Material Parameters

The parameters required for the material model used in FIAT are read from a material properties database file containing a number of ablators, high-temperature adhesives, and substructure materials. The model reads in parameters for virgin and char material states, applying those properties to the appropriate zones, and interpolates between the two states for TPS material that is in the pyrolysis zone. The level of pyrolysis is dictated by Eq. (2) and the supporting activation energy equation for thermal decomposition of TPS constituents. The material models used by FIAT are specifically tailored to each TPS material available in the database.

Parameter	
Virgin Density	ρ_v
Virgin Specific Heat	c_{p_v}
Virgin Thermal Conductivity	κ_v
Virgin Emissivity	ϵ_v
Char Density	ρ_c
Char Specific Heat	c_{p_c}
Char Thermal Conductivity	κ_c
Char Emissivity	ϵ_c
Char Blowing Rate	B'_c
Resin Decomposition	
Heat Transfer Blowing Correction	λ
Pyrolysis Gas Enthalpy	h_g

Table 1. PICA material model parameters carrying uncertainties.

III. Methodology

The following analysis is aimed toward guiding the MEDLI Material Properties Testing effort, which is tasked with precisely characterizing the TPS material used in the MISP plugs. Manufacturing imperfections, localized material variations, and other natural (aleatory) effects contribute to an inherent variability and uncertainty in the properties of the TPS material used in the MISP plugs. Given the small size of the plugs, these local effects could have significant effect on the thermal response and could in-turn affect the readings returned from the embedded instrumentation. Inaccurate characterization of MISP material properties will undoubtedly lead to errors in the analysis when using modeling and simulation software tools to perform the inverse analysis required to satisfy the MEDLI science requirements and could lead to erroneous conclusions on the accuracy of the underlying fitness of the predictive simulations used to model the entry phase of the mission.

Specific objectives for the MEDLI Material Properties Testing Effort are enumerated below, supported by questions that will guide the testing and analysis efforts.

1. Identify and Quantify Uncertainties in the material properties due to aleatory effects that could influence the inferences from the MEDLI data.
   (a) What distribution(s) best characterize the input parameters?
   (b) How are the input parameters related, and what is the best method of characterizing their relationship?
   (c) What are the contributions to the uncertainty in the TC reading solely from our lack of characterization of PICA material properties?
   (d) Which material properties are contributing most to our uncertainty in the TC readings?
2. Construct a revised PICA material model based on "area-averaged" material properties to capture the nominal response of a PICA-based TPS for design and analysis of future planetary exploration missions.
   (a) To a certain confidence measure, how accurately can we capture the bulk properties of PICA, and how do these uncertainties affect our assessments of heatshield performance?

To address the objectives and guiding questions outlined above, a three step analysis approach is proposed. Each step is intended to uncover a different aspect of how the predictive simulation responds to the anticipated flight environment and how the materials test plan can be structured to reduce the uncertainty in the simulation. The first step is guided toward a fundamental understanding of how perturbations in material properties affect the output simulated thermocouple temperature readings. The second will highlight how uncertainties in the material properties propagate through the analysis to result in TC temperature variability, tracing back that output uncertainty to specific sources of input uncertainty. The third step will reveal how changes in the assumed input uncertainties manifest themselves as changes to the output

uncertainty, thus providing the guidance necessary to target specific material parameters in the proposed material testing effort. The methodology for the three step procedure is outlined below.

1. Perform a deterministic sensitivity analysis to identify the material properties that have the most effect on the observed TC reading.

2. Assign probability density functions to the input parameters in accordance with our current level of knowledge of material properties based on other NASA test series and perform a sampling-based UQ analysis. Attribute simulated TC reading variability to specific sources of input variability using correlation coefficients and/or mutual information theory.

3. Train a surrogate model to mimic FIAT predicted TC outputs and perform numerous sampling-based UQ analyses, varying individual input PDF variances to determine quantitatively how changes in the assumed input PDFs track to changes in predicted TC variance.

A. Sensitivity Analysis

The sensitivity analysis is targeted specifically at identifying which material properties most affect the predicted thermocouple temperature reading for a specified aerothermal environment corresponding to a predicted MSL entry trajectory. Thermocouple temperatures are dependent on spatial location on the heatshield and depth within the PICA; they are driven by the various physical phenomena occurring in the PICA as it pyrolyzes and ablates in response to the imposed heating. As a consequence, the sensitivity of the thermocouple temperature reading to the various material properties will also be dependent on location and time. Characterizing this sensitivity will inform MEDLI analysts on how changing input parameters affect the FIAT TC readings and will be critical when reconciling any discrepancies between experimental/flight data and FIAT simulations.

Unfortunately, the architecture of FIAT does not currently support the use of complex numbers without significant modification to the source code, so a sensitivity analysis based on the complex-step method is not possible at this time. Automatic Differentiation remains as an option, and will be explored for the final paper.

The sensitivity analysis presented here is based on a finite-difference approach, with FIAT used only as a "black-box" in the calculation. Step size for the sensitivity study was assigned based on a convergence study testing three candidate step-sizes (5%, 1%, 0.1% of parameter nominal value) and two FIAT convergence levels for MISP 3. Results, shown in Fig. (3), indicate that numerical noise is present in the sensitivities at the smallest step size, while the largest step size loses some of the finer details of the simulation (though still capturing the dominant parameters). The tighter convergence does not seem to affect the results, but adds significant time to the computation and is deemed unnecessary. Sensitivity study preliminary results shown in subsequent sections utilize a step size of 1% and standard convergence settings in FIAT.

B. Uncertainty Quantification Analysis

The uncertainty quantification effort incorporates the current levels of confidence in the characterization of the various material properties and how those uncertainties propagate forward through FIAT resulting in a spread of temperature readings at each thermocouple at each MISP location. Where the finite-difference approach gives a raw measure of how perturbations in parameters affect output readings, the UQ analysis is aimed at understanding how our knowledge (or lack of knowledge) of particular parameters affect the simulated output data. Furthermore, by attributing TC temperature variability to variability in the input parameters, either through a correlation coefficient or analysis through mutual information theory, conclusions can be drawn as which input uncertainties are dominating the uncertainty in the predicted output. This information will guide the planning and execution of the MEDLI Material Properties Testing program, targeting those properties that are most at fault for the predicted thermocouple temperature variability.

Prior to performing the UQ analysis, it is important to characterize the appropriate inputs for the material properties. Which probability density functions best characterize the various parameters? The input parameters are known to be dependent on one another, what is the best method of characterizing this dependence? How many samples are required to identify parameter PDFs and dependencies? Preliminary analysis addresses this question with a Pearson's χ^2 distribution test, but will be supplemented or replaced by a more sophisticated Bayesian Inversion procedure.

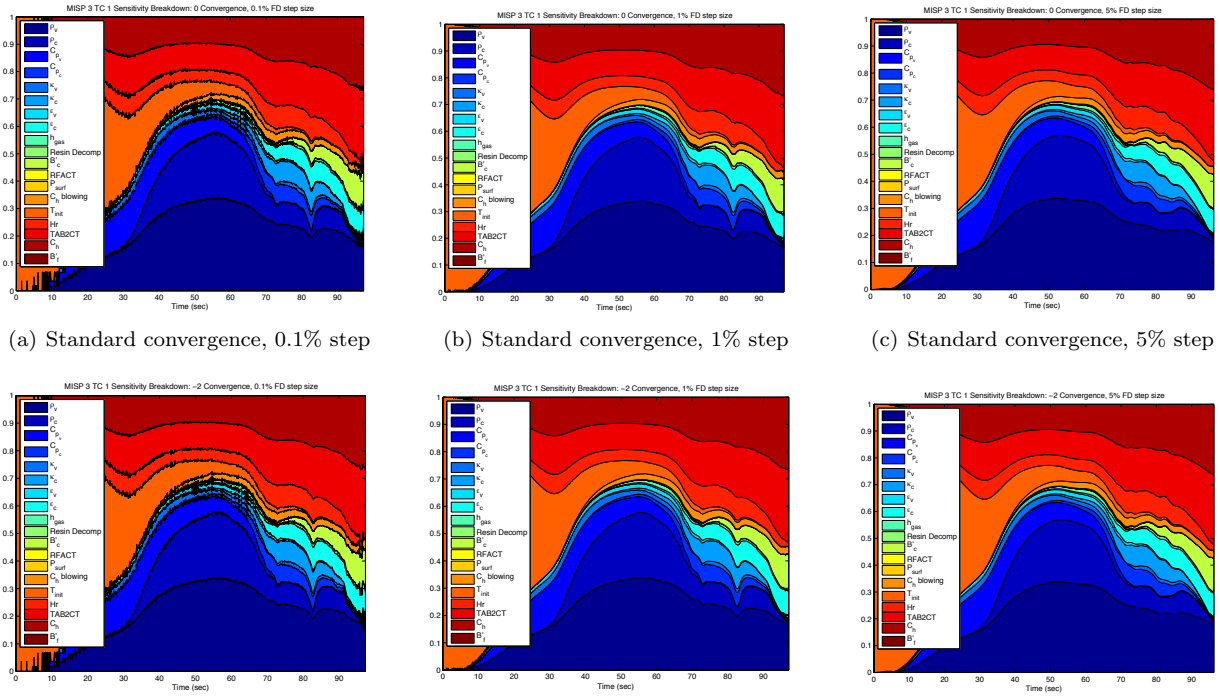

(a) Standard convergence, 0.1% step (b) Standard convergence, 1% step (c) Standard convergence, 5% step

(d) Tight convergence, 0.1% step (e) Tight convergence, 1% step (f) Tight convergence, 5% step

Figure 3. MISP 3 TC1 Finite-Difference Convergence Study.

Quantifying the consequences of a mis-prediction in the input parameter probability density functions will be accomplished via a comparison between a Monte Carlo analysis using normal distributions and uniform distributions with the same means and standard deviations. The outcome of the study will dictate the need (or lack thereof) to dedicate significant levels of funding in the Material Test Plan to accommodate many repeated tests required for reliability in the input PDF prediction and depends on the influence that the PDF tails have on the spread of the simulated output TC temperature readings.

The UQ analysis itself will be performed using a Monte Carlo based approach, whereby samples from the PDFs dictated in the steps above will be drawn and run through FIAT several thousand times to generate output statistics for each thermocouple at each MISP location for each time step.

Table 2. PICA Material Property PDF Uncertainties

Parameter	$2\sigma/\mu$
ρ_v	$\pm.075$
c_{p_v}	$\pm.05$
κ_v	$\pm.15$
ϵ_v	$\pm.03$
ρ_c	$\pm.10$
c_{p_c}	$\pm.10$
κ_c	$\pm.15$
ϵ_c	$\pm.05$
B'_c	$\pm.04$
Resin Decomp	$\pm.20$
λ	$\pm.15$
h_g	$\pm.20$

The final step in the UQ analysis will be the linking TC temperature uncertainty to the uncertainties in the input parameters. Preliminary analysis will utilize a correlation coefficient based approach due to its simplicity in implementation. To better characterize the relation between input and output uncertainties, mutual information theory or ANOVA decomposition will be applied. The comparison between the results of the correlation coefficient analysis and mutual information/ANOVA analysis will provide insight to any non-linearity in the FIAT models and will be important in characterizing whether the more sophisticated mutual information analysis technique will be necessary for future studies at the given aerothermal conditions.

C. Stochastic Sensitivity Analysis

The preceeding UQ analysis provides FIAT output statistics according to the assumed input distributions. This approach is acceptable under the assumption that the input distributions collected from the experimental measurements matches the true material property distributions. We expect this to be the case for very large sample sizes, but such large sample sizes of experimental data are not possible given the expense required to run arc jet tests. This effort is directed toward understanding the consequences of mis-predicting the parameters of the input PDFs by a small amount due to natural variability in the estimators of PDF parameters based on finite experimental population sizes.

A secondary benefit to the stochastic sensitivity analysis applies to the efforts of creating an "area-averaged" revised PICA material model. This model, to be based on the means from the samples of the various material properties collected during the ground test effort, will also see an inherent variability arise in the estimators for the means of these material properties according the the Central Limit Theorem. As sample sizes increase, estimators for the material property averages will converge to the true average with $\mathcal{O}(\sqrt{n})$. The stochastic sensitivity analysis will identify (in conjunction with, and supported by the previous two steps in the analysis) how an investment in additional testing buys refininement the material model.

The stochastic sensitivity analysis will be accomplished through a sequence of Monte Carlo based UQ propagation analyses with perturbations to the assumed input PDF parameters. Perturbations in output TC statistical properties will be recorded and a comparison to the baseline UQ analysis in the previous section will link cause and effect to perturbations in the input PDFs.

Performing these repeated sampling-based approaches will not be feasible without the use of a surrogate model for the FIAT runs to generate output statistics with enough reliability to draw reasonable conclusions from the results. A Kriging surrogate model will be constructed based on collected Monte Carlo results generated for the UQ analyses in the previous effort and sampling for the input PDF perturbation will be fed to the surrogate, permitting many repeated tests while collecting many thousands of output samples for reliable statistics. Validation of the surrogate will occur through spot-checking and comparison between surrogate and FIAT runs.

IV. Preliminary Results

A. Finite-Difference Sensitivity Analysis

The finite-difference sensitivity analysis for MISP locations 3 & 4 at each thermocouple locations are shown in Fig. (4) and Fig. (5) respectively. The stacked-area plots show the relative sensitivity of the TC temperature to the 11 material property inputs to FIAT. For a given vertical slice along the x-axis, the fraction of color belonging to parameters indicate how significant those parameters are at that time step. For an example, see Fig. (4a). The sensitivity of TC1 temperature at MISP 3 to char density is zero until the onset of char formation 33 seconds past entry interface where it then contributes significantly to the sensitivity of the TC reading. Note the time axis on Fig. (4a) differs from the other subfigures due to the burnout of the thermocouple as the TPS material recedes beyond its in-depth location in the plug.

What is also interesting to note are the dissimilarities between Fig. (4) and Fig. (5) due to the drastically different aerothermal environment experienced by the two different plugs. MISP 3, located in the turbulent region experiencing the highest heating rates shows noticeably different behavior than at the stagnation point recorded by MISP 4. This highlights the importance of the MISP sensor placement in the heatshield and the need for a systematic approach for comparing the predictions at the different sensor placements. Potential discrepancies between flight data recorded by the MEDLI system and the predictive FIAT simulations could be caused by inaccuracies in different input parameters, depending on spatial location on the heatshield, complicating the post-flight data analysis.

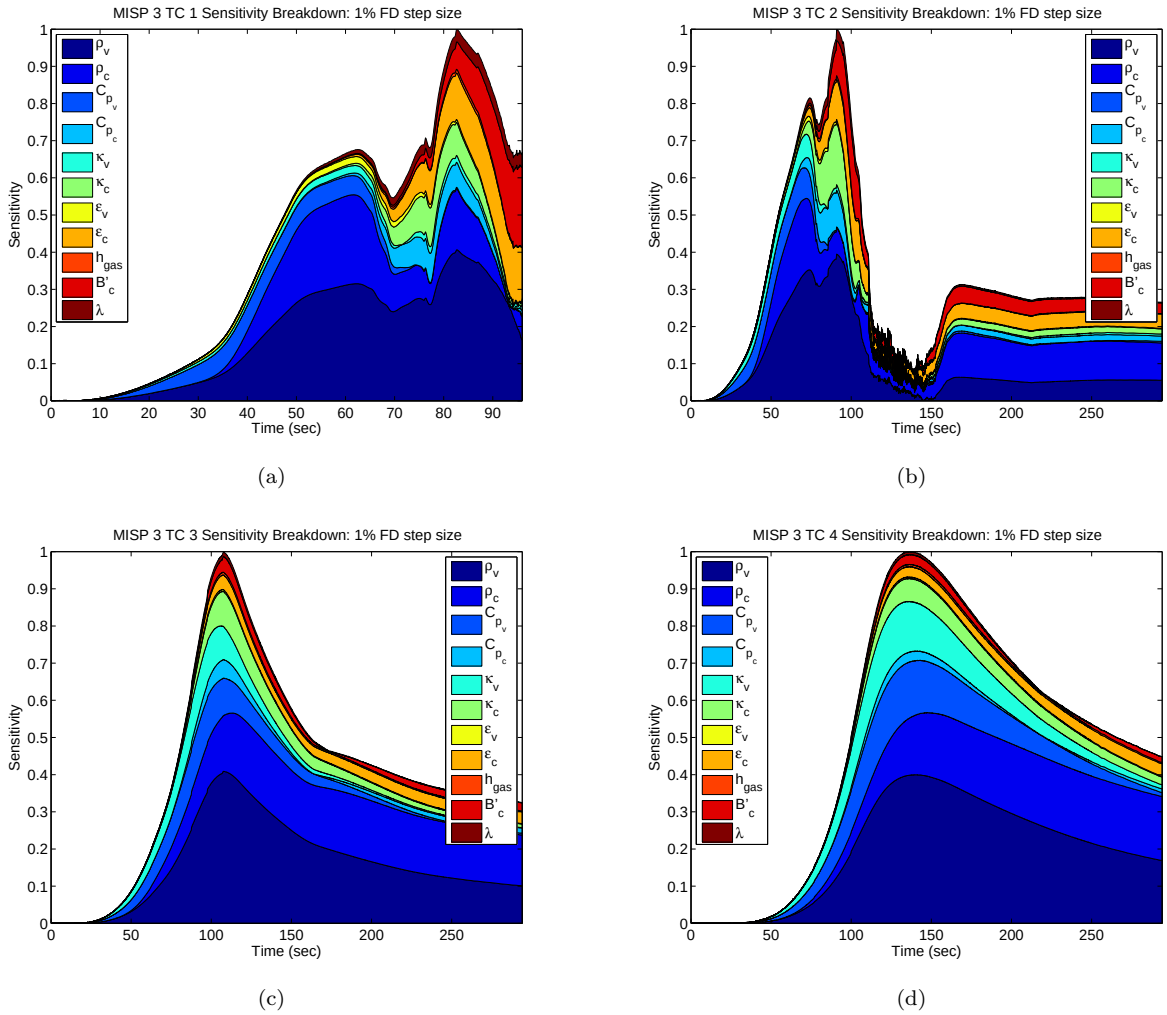

Figure 4. MISP 3 Finite-Difference Sensitivity Analysis.

B. Uncertainty Quantification

Prior to executing the UQ runs, a study was undertaken to try and identify how many repeated samples would be necessary to isolate the statistical distributions from which the samples were drawn. This is targeted specifically for trying to identify the appropriate input distributions for the various material properties in the UQ analysis and whether identifying those PDFs could be within the scope of the material testing plan. This study used a Pearson's χ^2 Distribution test and an Anderson-Darling test to compare the observed samples to a known distribution specified as the null hypothesis. A set of 2000 statistical tests were performed for sample sizes between 10 and 200, and statistical test mis-prediction rates were collected (Type I or Type II errors). Results for this study show (approximately) how many repeated samples of a particular property would be necessary to reliably conclude that the outcome of the statistical test comes to the correct conclusion. Results for this preliminary analysis are shown in Figs. () and ().

The outcome of this preliminary analysis shows that to avoid making Type II errors with a reasonable level of confidence, $\mathcal{O}(10^2)$ repeated samples are necessary. Such a commitment may be possible for virgin material properties that do not require the use of an arcjet facility, but are prohibitively expensive for the PICA char properties.

Preliminary UQ runs for normally and uniformly distributed inputs with parameter standard deviations defined in Tab. (2) for 2000 FIAT runs each are shown in Fig. (7) at MISP 3. TC mean values for each time step are shown in solid lines and a band of two standard deviations is enclosed in the dotted lines. As mentioned in the previous section, the top two thermocouples (shown in black and blue respectively) burn

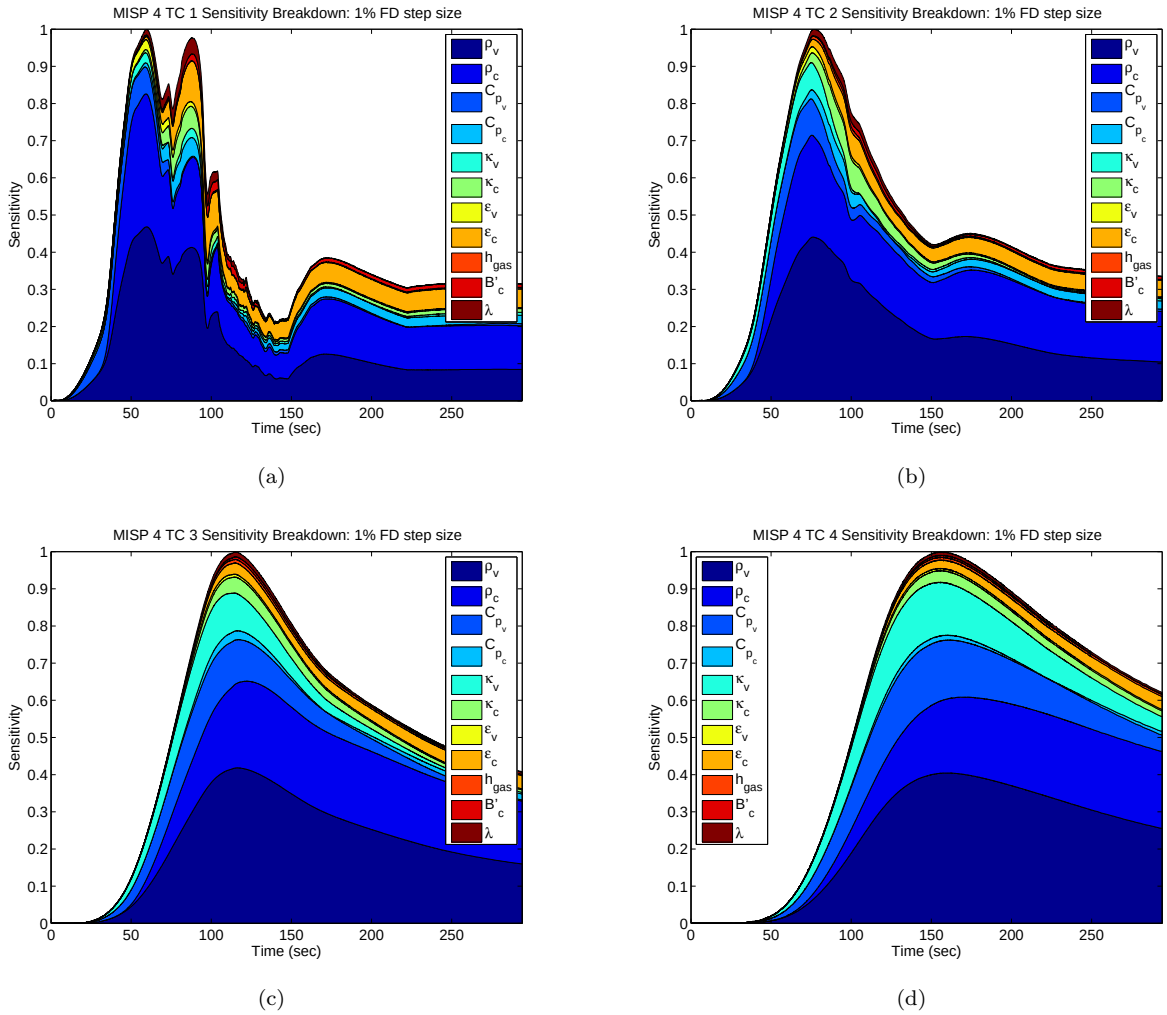

Figure 5. MISP 4 Finite-Difference Sensitivity Analysis.

out as the recession of the TPS material exceeds the TC in-depth plug location.

Interesting to note is the lack of significant variation in the predicted standard deviations between the two different input PDF sets. An overlay of the two results is shown in Fig. (B) and the envelopes for 2σ are virtually indistinguishable. Based on this preliminary analysis, the tails of the input PDFs for the material properties do not measurably affect the variation in the TC reading. As such, it is not necessary to spend the significant effort and money to generate the large sample sizes required to reliably predict input distributions according to Pearson's χ^2 Distribution Test.

C. Stochastic Sensitivity Analysis

Preliminary results for the stochastic sensitivity analysis are forthcoming but are unavailable at this time.

V. Remaining Work

Many of the analysis steps proposed in the Methodology have been worked through for simulated data collected at a single MISP location. Some comparison work between stagnation point sensitivities and turbulent region temperature sensitivities has been undertaken, with other MISP location comparisons underway. Statistical data has been collected for the MISP 3 UQ analysis, and must be completed for the other MISP locations. The breakdown of uncertainty contributors via correlation coefficients/mutual information/ANOVA is a key component of the UQ analysis and still remains to be completed. The stochastic sensitivity analysis

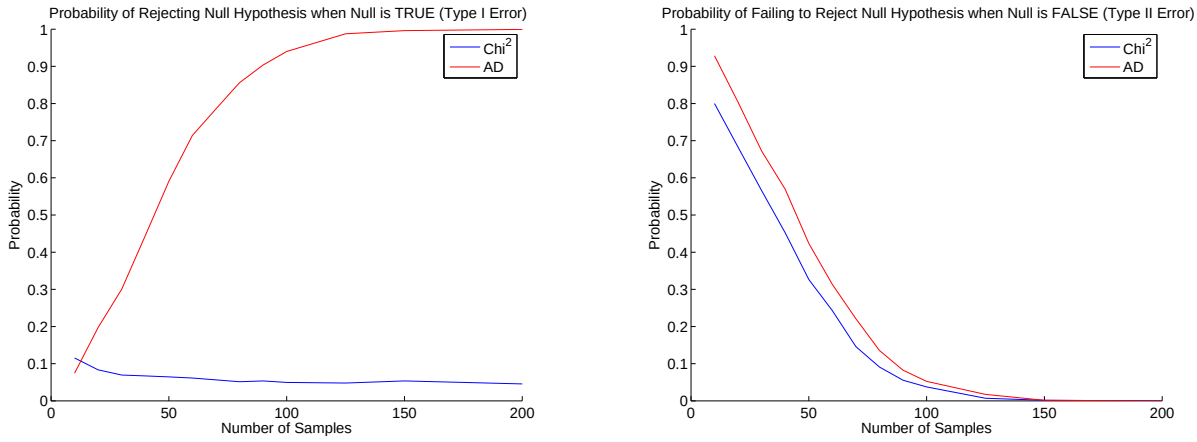

(a) (b)

Figure 6. Statsitical test mis-prediction rates (Type I and Type II errors) for given sample sizes.

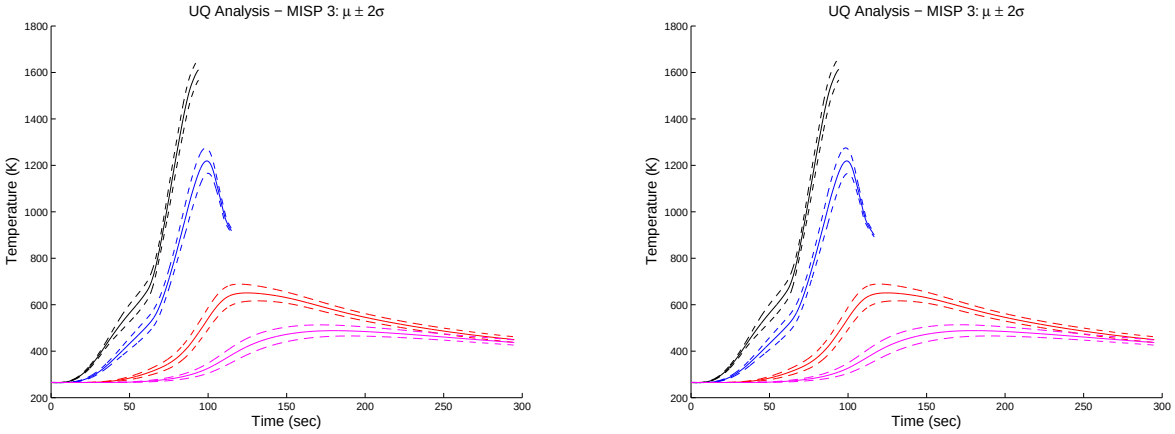

(a) Normal Distributions (b) Uniform Distributions

Figure 7. MISP 3 Uncertainty Quantification Analysis Using Differing Input Distributions.

via Kriging surrogate model for FIAT is also at an early stage, with completion and validation required. In the final version of the paper, we expect to include the following

1. Sensitivity analysis results for the 7 MISP locations, each with 4 in-depth TCs (via current finite-difference based approaches or through Automatic Differentiation).
2. Uncertainty quantification showing the variability in the simulated TC temperature readings at each MISP location.
3. UQ decomposition in time for each MISP/TC group showing time-dependent rankings of primary uncertainty contributors during the simulated entry mission.
4. Stochastic sensitivity analysis results showing the effect of perturbations in input PDFs on output statistics.

Through the results enumerated above, we hope to identify and rank primary sources of uncertainty from material properties in a flight-relevant environment, to show the dependence on spatial orientation and in-depth location on those uncertainty contributors, and to quantify how sensitive the expected results are (indirectly specifying the scale of the material properties experimental test effort by dictating the number of required repeated samples to achieve desired accuracy in output statistics).

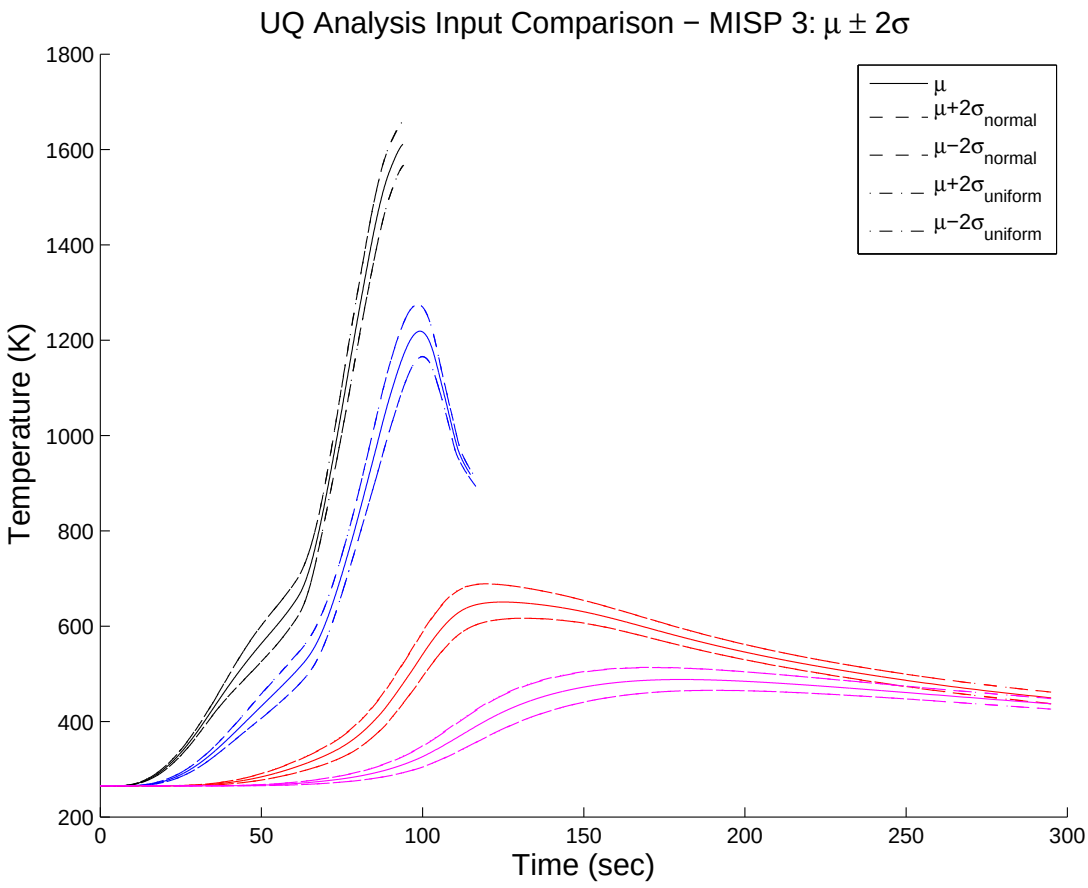

Figure 8. MISP 3 Input PDF Overlay

Acknowledgments

The authors would like to thank the MEDLI program by which this research was funded. Sean R. Copeland would like to thank the Lillie family for their generous support of the Stanford Graduate Fellowship program. Additionally, the input and suggestions to this research from Karthik Duraisamy, Deepak Bose, Milad Mahzari, and Paul George Constantine are greatly appreciated.

References

[1]Anderson, J. D., *Hypersonic and High-Temperature Gas Dynamics*, AIAA Education Series, Reston, 2006.

[2]Rasmussen, C. E., and Williams C., *Gaussian Processes for Machine Learning*, MIT Press, Cambridge, 2006.

[3]Gazarik, M., Wright, M., Little, A., Cheatwood, F., Herath, J., Munk, M., Novak, J., and Martinez, E., Overview of the MEDLI Project, IEEE Aerospace Conference, Big Sky, MT, No. IEEEAC paper No. 1510, 2008.

[4]Wright, M. J., et. al, "A Review of Aerothermal Modeling for Mars Entry Missions", *AIAA 2010-443*, 48th AIAA Aerospace Sciences Meeting Including the New Horizons Forum and Aerospace Exposition, Orlando, FL 2010.

[5]Chen, Y.-K., and Milos, F. S., Fully Implicit Ablation and Thermal Analysis Program (FIAT), *ICCE/4, Fourth International Conference on Composites Engineering*, edited by D. Hui, International Community for Composites Engineering and College of Engineering, Univ. of New Orleans, New Orleans, LA, 1997, pp. 661, 662.

[6]Chen, YK., Milos, F.S., Ablation and Thermal Response Program for Spacecraft Heatshield Analysis, Journal of Spacecraft and Rockets, Volume 36, Number 3, May-June 1999.

[7]Moyer, C. B., and Rindal, R. A., An Analysis of the Coupled Chemically Reacting Boundary Layer and Charring Ablator, Part II, Finite Difference Solution for the In-Depth Response of Charring Materials Considering Surface Chemical and Energy Balances, NASA CR-1061, June 1968.

[8]Users Manual: Aerotherm Charring Material Thermal Response and Ablation Program, Aerotherm Div., Acurex Corp., Mountain View, CA, Aug. 1987.

[9]Cozmuta, I., et. al, "Defining Ablative Thermal Protection System Margins for Planetary Entry Vehicles", *AIAA 2011-3757*, 42nd AIAA Thermophysics Conference, Honolulu, HI 2011.

[10]White, T., et. al, "Proposed Analysis Process for Mars Science Laboratory Heat Shield Sensor Plug Flight Data", *AIAA 2011-3957*, 42nd AIAA Thermophysics Conference, Honolulu, HI 2011.